

Journal of Materials Chemistry C

Accepted Manuscript



This article can be cited before page numbers have been issued, to do this please use: M. Li, Y. Wang, J. Wang and Y. Chen, *J. Mater. Chem. C*, 2017, DOI: 10.1039/C7TC00173H.



This is an Accepted Manuscript, which has been through the Royal Society of Chemistry peer review process and has been accepted for publication.

Accepted Manuscripts are published online shortly after acceptance, before technical editing, formatting and proof reading. Using this free service, authors can make their results available to the community, in citable form, before we publish the edited article. We will replace this Accepted Manuscript with the edited and formatted Advance Article as soon as it is available.

You can find more information about Accepted Manuscripts in the [author guidelines](#).

Please note that technical editing may introduce minor changes to the text and/or graphics, which may alter content. The journal's standard [Terms & Conditions](#) and the ethical guidelines, outlined in our [author and reviewer resource centre](#), still apply. In no event shall the Royal Society of Chemistry be held responsible for any errors or omissions in this Accepted Manuscript or any consequences arising from the use of any information it contains.

(Z)-Tetraphenylbut-2-ene-1,4-diones: Facile Synthesis, Tunable Aggregation-Induced Emission and Fluorescence Acid Sensing

Mengwei Li,[†] Yi-Xuan Wang,[†] Jianhui Wang* and Yulan Chen*

Received 00th January 20xx,
Accepted 00th January 20xx

DOI: 10.1039/x0xx00000x

www.rsc.org/

A facile approach to synthesize stereospecific (Z)-aryl functionalized 1,4-enediones was presented. The resulting molecules (TPBD-1, TPBD-2) have been demonstrated as a new type of heteroatoms-containing AIE-active luminogens with multiple sites for structural modifications. Knoevenagel reaction of TPBD-1 led to the high electron affinity cyano derivative (TPBD-CN), which showed enhanced AIE performance and pronounced red-emission. More interestingly, TPBD-1 exhibited acid-induced red emission both in dilute solution and in solid state, which was attractive owing to its great potential for “turn on” optical sensing. The reversible fluorescence acid sensing can be attributed to the stepwise binding effect of carbonyl groups on the 1,4-enedione core to rigidify the molecular conformation and strengthen the D-A interaction, that was systematically investigated by UV-Vis, FL, FT-IR and NMR spectroscopy, and was further corroborated by DFT calculations.

Introduction

The last decade has witnessed an exponential increase in the development of luminescent materials for their potential applications in electronics, optics, biological science and sensors.¹ In contrast to the destructive effect of aggregation caused quenching (ACQ) derived from most conventional luminophores,² aggregation-induced emission (AIE) has made aggregation process productive in light emission, and thus opened new avenues to various possibilities for high-tech innovations.³ As pioneered by Tang and coworkers, AIE referred to a unique photophysical phenomenon that light emission of a luminogen is activated by the formation of aggregates. Propeller-like molecules such as siloles and tetraphenylethenes (TPE) were firstly identified as AIE-active luminogens.⁴ Later on, more experimental and theoretical analyses have consistently supported that the restriction of intramolecular motions (RIM) was the main cause for the AIE effect.^{3a,5} Up to now, enormous efforts have been devoted to the exploration of AIEgens with novel structures and versatile functionalities.⁶ For instance, incorporation of heteroatoms, like N, O, etc., into an AIEgen has become a promising strategy to fine-tune the photophysical properties of the luminogen. The heteroatoms can not only considerably alter the emission behaviours of the luminogen, particularly its color tunability, but also endow heteroatom-containing AIEgens with stimuli-responsibility beyond the AIE feature.⁷

1,4-Enediones have attracted great attention of organic chemists, since they constitute key components of many bioactive compounds.⁸ Besides, by virtue of their multifunctional composition, they can serve as excellent substrates for further synthetic elaboration. However, until now, 1,4-enediones have been rarely used as building block to construct optoelectronic materials, mainly due to their poor conjugation. While considered the structure feature, aryl-substituted 1,4-enediones can be regarded as a kind of sterically hindered molecules having an ethene core decorated with arylmethanone rotors. And compared to TPE, the additional carbonyl groups would lead to new heteroatom-containing AIE-active luminogens with multiple sites for structural modifications, tunable optical properties and electron affinity. Herein, we reported the Z-selective synthesis of a series of (Z)-1,4-enedione derivatives (TPBD, Figure 1). By incorporating sterically demanding phenyl groups, these tetra-substituted (Z)-1,4-enediones are AIE active and display reversible fluorescence emission in response to acid and basic switching, thus enabling them to perform not only as promising optical pH sensors in solution, but also fluorescent detectors for acidic and basic vapor in solid state. Furthermore, derivatization of the (Z)-1,4-enedione to its malononitrile counterpart (TPBD-CN, Figure 1) demonstrated it as a versatile building block to create redder light emitters.

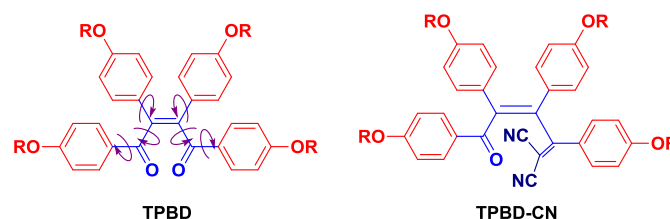


Figure 1. Chemical structures of TPBDs and TPBD-CN in this work.

Tianjin Key Laboratory of Molecular Optoelectronic Science, Department of Chemistry, Tianjin University, Tianjin, 300354, P. R. China.

*E-mail: yulan.chen@tju.edu.cn; wjh@tju.edu.cn

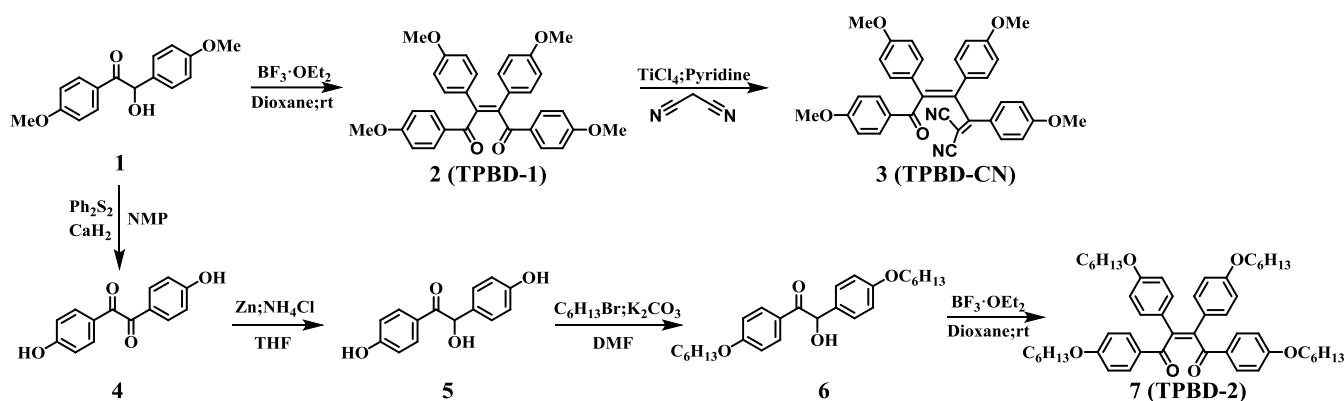
[†] The authors contributed equally to this work.

Electronic Supplementary Information (ESI) available: Synthetic procedures, experimental details, ¹H NMR and ¹³C NMR spectra, MALDI-TOF spectra, crystal data of TPBD-1, DLS data, more UV-Vis absorption and PL spectra, DFT calculation results. See DOI: 10.1039/x0xx00000x

Results and Discussion

The structures and synthetic routes of (*Z*)-tetraphenylbut-2-ene-1,4-diones **TPBD-1** and **TPBD-2** in this work are depicted in Scheme 1. The ethene core in **TPBDs** is embellished with two phenyl rings and a pair of phenylmethanone groups. According to the reported strategies towards 1,4-enedione derivatives, special and elaborate reaction conditions were usually required.⁹ Herein, we found a quite straightforward way leading to stereospecific (*Z*)-1,2,3,4-tetraphenylbut-2-ene-1,4-dione derivatives (**TPBDs**) by dimerization of their benzoin precursors under mild condition. Taking **TPBD-2** for example, starting from the commercially available 2-hydroxy-1,2-bis(4-methoxyphenyl)ethanone (**1**), $\text{CaH}_2\text{-Ph}_2\text{S}_2$ in NMP was chosen as an efficient protocol for deprotection of methyl groups, concomitant with the oxidation of its hydroxyl group to afford 4,4'-dihydroxybenzil **4** (yield: 85%).¹⁰ Bis-hexyloxy

functionalized benzoin **6** was obtained by reduction of **4** and followed by Williamson etherification with 1-bromohexane. Optimal conditions for dimerization were then estimated through a series of screening experiments. By using 1,4-dioxane as the solvent and $\text{BF}_3\cdot\text{OEt}_2$ as the catalyst, **TPBD-2** could be synthesized in one-step at room temperature in 60% yield. **TPBD-1** was prepared in a similar way. The plausible mechanism for dimerization was proposed in Scheme S1. **TPBDs** could be readily derived to intramolecular charge-transfer (ICT) compound by incorporating the electron-deficient cyano groups via Knoevenagel condensation. For instance, treatment of **TPBD-1** with malononitrile, TiCl_4 and catalytic amount of pyridine in dry 1,2-dichloroethane accomplished **TPBD-CN** in a yield of 36%. All the compounds were unambiguously characterized with ^1H and ^{13}C NMR spectra, and matrix-assisted laser desorption ionization time-of-flight (MALDI-TOF) mass spectroscopy.



Scheme 1. Synthetic routes to **TPBDs** and **TPBD-CN**.

The single crystal of **TPBD-1** was obtained by slow evaporation of its dichloromethane/diethyl ether solution. Figure 2a confirmed the stereospecific feature of the dimerization reaction of benzoin, through which the 1,4-enedione core of **TPBD-1** adopted *Z*-type conformation in the solid state. Moreover, **TPBD-1** exhibited a highly twisted propeller-like geometry with large twisting angles in the range of 38° to 73°. As presented in Figure S1, the packing diagram of **TPBD-1** showed that the molecules stacked in an antiparallel style with large side-slipping, driven by multiple intermolecular interactions, such as $\text{C-O}\cdots\text{H-C}$ and $\text{C=O}\cdots\text{H-C}$ hydrogen bonds, as well as $\text{C-H}\cdots\pi$ interactions, with distances in the range of 2.4–3.1 Å (Figure 2). The multiple intermolecular interactions rigidified the molecular structure in the crystal lattice, which was expected to prevent excitons from a non-radiative dissipation. The distance between antiparallel phenyl rings of the adjacent molecules is as large as 5.4 Å, indicating the absence of $\pi\cdots\pi$ stacking interactions. Therefore, ACQ effect, generally caused by tight π -stacking, might be suppressed in the crystal state of **TPBD-1**. Unfortunately, the single crystal of **TPBD-CN** was not available, probably caused by the increased steric hindrance from the two cyano groups located closed to the carbonyl group.

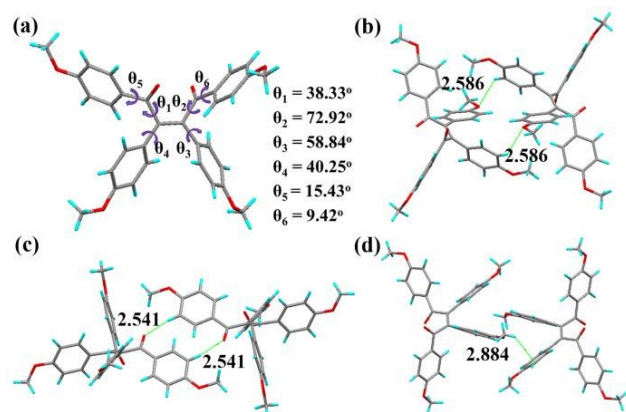


Figure 2. (a) Single crystal structure and torsion angles of **TPBD-1**. Multiple intermolecular interactions existed in the crystal, including (b) $\text{C-O}\cdots\text{H-C}$ hydrogen bond, (c) $\text{C=O}\cdots\text{H-C}$ hydrogen bond, and (d) $\text{C-H}\cdots\pi$ interaction.

The electronic distribution of HOMO and LUMO energy levels of **TPBD-1** and **TPBD-CN** were studied theoretically by density functional theory (DFT) calculations at the level of B3LYP/6-31G*. As shown in Figure 3, electrons of both

molecules are delocalized over the conjugated diphenylethene cores in the ground state. While they turn to be distributed over the benzoyl groups for **TPBD-1**, and cyano groups as well as the adjacent phenyl rings for **TPBD-CN**, indicative of ICT characters. The calculated bandgap of **TPBD-CN** is lower than that of **TPBD-1**, resulted from the appended cyano groups which simultaneously enhanced the π -conjugation and the D–A interaction in **TPBD-CN**.

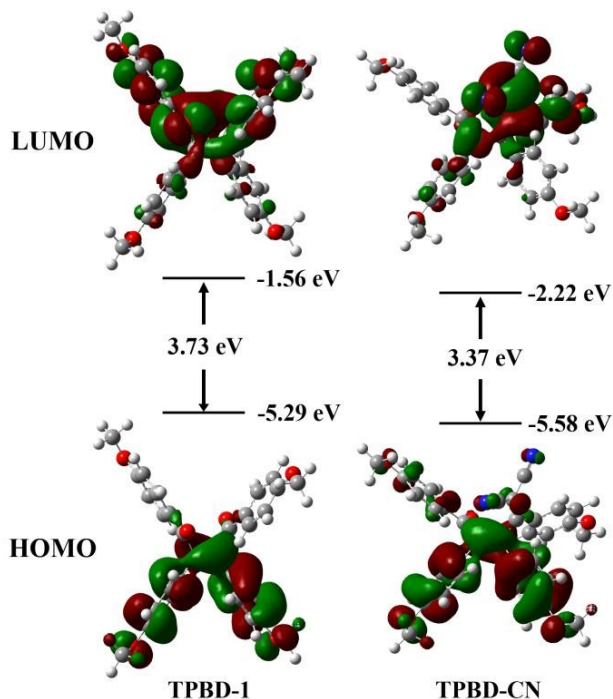


Figure 3. Molecular-orbital amplitude plots and energy levels of the HOMOs and LUMOs for **TPBD-1** and **TPBD-CN** in the gas phase, as calculated at the level of B3LYP/6-31G*.

Since highly twisted configuration and dense intermolecular hydrogen bonds were found in **TPBD-1** crystal, both of which were critical factors responsible for the restriction of intramolecular rotation, we were then interested in the photophysical properties of these **TPBD** based molecules. All the three molecules were soluble in common organic solvents, such as toluene, THF, DCM and DMF, and exhibited no obvious solvent effect (Figure S2). In dilute THF solution, the maximum absorption of **TPBD-1** and **TPBD-2** was located at 287 nm, with an ambiguous shoulder peak at ca. 340 nm, which became much stronger in the case of **TPBD-CN** (Figure 4a). The shoulder peak could be ascribable to the ICT transition, suggesting that the absorption of chromophore was successfully tuned via derivatization of 1,4-enedione cores to incorporate strong electron withdrawing groups. In THF/water mixture with a water fraction (v/v , f_w) of 95%, the absorption peaks of **TPBD-1**, **TPBD-2** and **TPBD-CN** all shifted bathochromically and became broadened (Figure S3), due to the formation of nanoaggregates with hydrodynamic diameters as large as hundreds of nanometers, as verified by dynamic light scattering experiments (Figure S4).¹¹

All the three molecules are non-fluorescent in dilute THF solution while exhibit AIE characters with different emission colors. For instance, the fluorescence spectra of **TPBD-1** remained unchanged in mixed solution of THF/water until the f_w reached about 80% (Figure 4b, S5 and S6). Upon further increasing f_w , an intense emission peak at 500 nm appeared, with fluorescence quantum yield of 2.53% (Table S1), that is, 42 times higher than that in isolated state ($\Phi_F = 0.06\%$). The spectrum in the film state was almost identical to that in THF/water mixture solution, showing green fluorescence emission. Whereas for its crystalline state, the emission band blue-shifted remarkably with a maximum peak at 460 nm (Figure 5a). The corresponding Φ_F value was estimated as 2.33% with a fluorescence lifetime of 0.90 ns (Figure S7a, Table S2). Since the twisting motions in crystalline molecules can be inhibited more pronouncedly during ordered arrangement than those in amorphous states (i.e., analyses of nanoaggregates and films, supported by XRD results shown in Figure S8), it is reasonable that the molecular reorganization energy in crystals is lower than that in amorphous film, resulting in a blue-shifted emission.¹² **TPBD-2** bearing peripheral alkyl chains exhibited similar photophysical properties, with a 4-fold enhancement of Φ_F in THF/water mixture when f_w reached 95% ($\Phi_F = 0.37\%$), compared to the value in THF ($\Phi_F = 0.09\%$ in THF, Figure 4c and S9). It should be noted that **TPBD-2** could hardly become crystallized, suggesting that the long alkyl chains efficiently alleviated the intermolecular stacking. Therefore, the advanced AIE performance of **TPBD-1** over that of **TPBD-2** mainly arised from a stronger intermolecular stacking in the aggregate state.

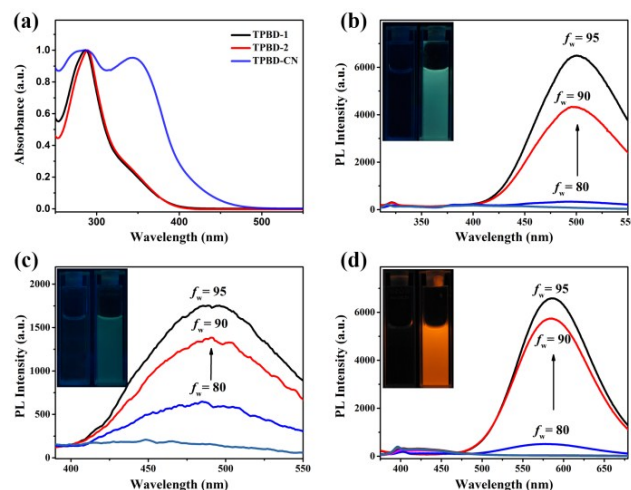


Figure 4. (a) UV-Vis absorption spectra of **TPBD-1**, **TPBD-2** and **TPBD-CN** in THF solution; Fluorescence spectra of (b) **TPBD-1**; (c) **TPBD-2** and (d) **TPBD-CN** in THF/water mixtures with different water fractions (concentration: 2×10^{-5} M; excitation wavelength for **TPBD-1**: 290 nm; for **TPBD-2**: 287 nm, and for **TPBD-CN**: 355 nm). Inset: Photographs of the corresponding molecules in THF (left) and THF/water mixtures ($f_w = 90\%$, right) under the illumination with 365 nm UV light.

As for **TPBD-CN** possessing inherent D–A structure, distinctive tunable emission were observed upon aggregation (Figures 4d, 5b and S10). Indeed, a strong and orange emission

band peaked at 585 nm was detected in the THF/water mixture ($f_w = 95\%$) of **TPBD-CN**, whose fluorescence quantum yield ($\Phi_F = 5.25\%$) was more than 100-fold higher than that in THF solution ($\Phi_F = 0.05\%$). And the Φ_F of **TPBD-CN** powder was estimated as high as 25.18% with a fluorescence lifetime of 6.04 ns (Table S1, S2), implying that the intramolecular motions were hampered more sufficiently in solid state.¹³ **TPBD-CN** possessed the most pronounced AIE properties among the three **TPBD**-based molecules, which can be ascribed to the significant role of cyano groups to afford a more hindered and twisted molecule configuration together with an extra pathway for the non-radiative excited-state decay via their vibrational motion.¹⁴ Delayed PL measurements were then conducted. Besides the fluorescence peak, a new peak at 625 nm was detected from the crystal of **TPBD-1**, which was assignable to room temperature phosphorescence (RTP, Figure S11).¹⁵ Neither the **TPBDs** solutions nor the **TPBD-CN** powder exhibited RTP, generally due to the poor crystallization capacity. Based on the above results, conclusions can be drawn as follows: (1) aryl-modified 1,4-enediones exhibit a typical AIE feature, and further substitution with cyano units endows the chromophore with red-shifted luminescence because of the strengthened D–A effect, as well as the better AIE performance caused by the additional mechanism of restriction of intramolecular vibration (RIV).¹⁶ (2) Compared to TPE, the presence of carbonyl groups can promote the RTP emission, particularly in the crystalline state.

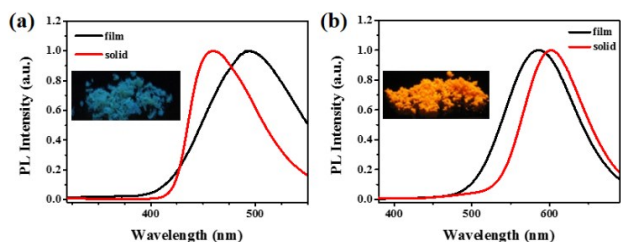


Figure 5. Fluorescence spectra of (a) **TPBD-1** and (b) **TPBD-CN** in film and solid state (excitation wavelength for **TPBD-1**: 290 nm; for **TPBD-CN**: 355 nm). Inset: Photographs of **TPBD-1** and **TPBD-CN** in solid state under the illumination with 365 nm UV light.

Intriguingly, **TPBD-1** exhibited considerable response to trifluoroacetic acid (TFA) in non/low polar solvents, such as hexane, toluene, DCM, and chloroform (Figure S12), all of which have weak ability to compete for protons.¹⁷ Titration experiments of **TPBD-1** with TFA were performed in chloroform (Figure 6). A new absorption peak at 500 nm appeared upon increasing TFA from 0 to 0.3 M, accompanied with a chromatic change of the transparent solution from colorless to yellow. Meanwhile, a bright PL emission peaked at 660 nm was “turned on”, and a 1000-fold increase of Φ_F from 0.01% to 11.34% was observed (Table S3), indicating a remarkable fluorescence sensing ability of **TPBD-1** for TFA. To illuminate the responsive mechanism, control experiments were performed as follows. Firstly, upon addition of triethylamine (TEA), the TFA-induced spectral changes recovered immediately, implying fast and reversible characteristics for such a response; Secondly, besides TFA, various acids, including H_2SO_4 , HCl, HNO_3 , and HCOOH , were

screened, which could efficiently trigger the optical changes as well (Figure S13), demonstrating that the response derived from the interaction of **TPBD-1** with proton, instead of CF_3COO^- . Since the carbonyl groups of **TPBDs** exhibited Lewis base properties, which could be strengthened by π -conjugation with 4-methoxyphenyl groups, 1,4-enedione units were deduced to act as binding sites to protons. As displayed in Figure S14, the FT-IR spectral changes observed upon titration of **TPBD-1** by TFA were associated with the complexation of carbonyl groups. The essential role of 1,4-enediones in the fluorescence sensing was further evidenced by testifying with **TPBD-CN**. Since one of the carbonyl groups had been substituted, the binding capacity of **TPBD-CN** was reduced, leading to a weaker tendency towards complexation with TFA. As shown in Figure S15, the UV-Vis absorption and PL spectra were almost invariant upon treatment with TFA and TEA. Moreover, the absorption band of acidified **TPBD-1** shifted bathochromically with the increase of solvent polarity (Figure S16), exhibiting a typical ICT character.^{7b} Combined with the proposed binding mode, we speculated that this unique absorption feature originated from the ICT process between 4-methoxyphenyl groups as electron donating units and protonated 1,4-enediones as efficient electron withdrawing parts.

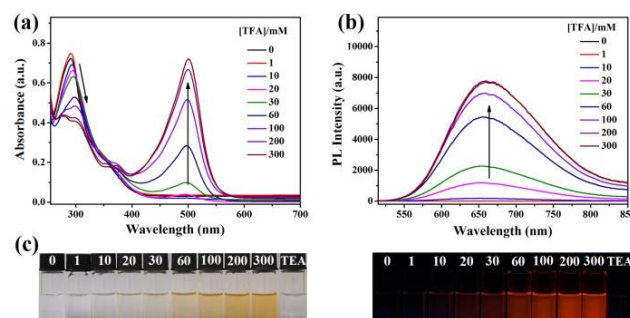


Figure 6. (a) UV-Vis absorption spectra and (b) fluorescence spectra of **TPBD-1** in chloroform with different concentrations of TFA. (c) Photographs of all the above samples and the acidified solution upon further treatment with TEA in chloroform (taken under both natural light and the illumination with 365 nm UV light). Concentration of **TPBD-1**: 2×10^{-5} M, excitation wavelength: 500 nm.

NMR measurements were carried out to shed more light on the complexation behavior at a molecular level. After the addition of excess TFA (200 equiv.), chemical shifts (δ) of the aromatic protons and carbonyl carbon of **TPBD-1** showed striking changes (Figure 7a, b), whereas the signals of **TPBD-CN** shifted only slightly under the same conditions (Figure S17), suggestive of more significant variation in molecular configuration of **TPBD-1**–TFA complex than that of **TPBD-CN**–TFA with carbonyl units performed as efficient binding sites. Additionally, ^1H NMR spectra of **TPBD-1**–TFA complexes with different molar ratios were measured to identify the binding stoichiometry.¹⁸ As shown in Figure 7c, the peak at 7.12 ppm firstly underwent upfield shifts with increasing the molar fraction of TFA, but shifted inversely when the fraction was above 0.5, probably attributed to the presence of different

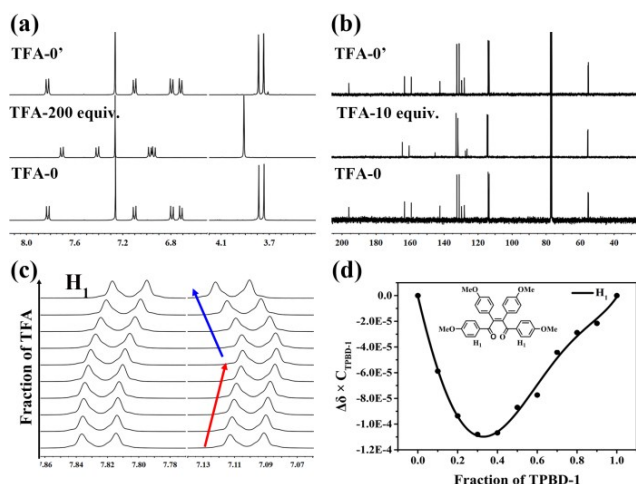


Figure 7. (a), (c) ^1H NMR spectra of **TPBD-1** (5 mM) in CDCl_3 after the addition of TFA (200 equiv.). (b) ^{13}C NMR spectra of **TPBD-1** (50 mM) in CDCl_3 after the addition of TFA (10 equiv.). (d) A Job plot of "H1" for **TPBD-1** upon combination with TFA. ($[\text{TPBD-1}] + [\text{TFA}] = 30 \text{ mM}$, 400 MHz, 298.15 K). TFA-0': NMR spectra measured after removal of TFA under vacuum.

states for **TPBD-1**–TFA complexes. An inflexion was observed in the Job plot (Figure 7d), which was obtained by monitoring the peak at ca. 7.84 ppm, clearly confirming a 1:2 binding stoichiometry of **TPBD-1** with TFA. Thus, the two carbonyl groups of **TPBD-1** were deduced to be protonated stepwise by TFA. DFT calculations showed that the molecular conformation of the 1:2 complex was highly distorted and thus fixed by the boosted intramolecular tension (Figure S18a), possibly originated from the strong electrostatic repulsion between the cationic units. Additionally, the charge transfer from 4-methoxyphenyl group to protonated 1,4-enedione upon excitation, and the reduced bandgap of such complex jointly supported that the TFA-mediated absorption derived from an ICT effect (Figure S18b). The proposed protonation mechanism was depicted in Scheme S2, through which the protonated **TPBD-1** could be stabilized with quinoid resonance structure, as was, on the other hand, confirmed by DFT calculation showing shortened length of C–O (OCH_3) bond after protonation. Since the TFA-treated **TPBD-1** did not form nanoaggregates in solution (absence of Tyndall effect as shown in Figure S19), the corresponding PL emission should also be ascribed to the more rigid structure of the **TPBD-1**–TFA complex. All the TFA-induced variations in NMR, UV-Vis and PL spectra were eliminated by removing TFA under vacuum (Figure 7a, b), demonstrating the good stability of **TPBD-1** and the reversibility of TFA binding.

Combining all these results, a mechanism of TFA sensing was proposed: the two carbonyl groups of **TPBD-1** stepwisely bound with two protons from TFA; the resulted cationic 1,4-enediones twisted to reduce the intramolecular electrostatic repulsion and rigidified the whole molecule structure, as well as facilitated the ICT effect because of its promoted electron withdrawing ability; the ICT process implemented a new absorption band in the visible light range (at 500 nm), leading to the chromatic response, and the rigidified molecule

presented the intense emission at 660 nm through a RIM effect, resulting in the fluorescence response.

Taking advantage of the remarkable response capacity, **TPBD-1** was utilized to fabricate solid-state sensory material. The sensor was prepared by depositing **TPBD-1** on a piece of filter paper. After exposure in different acid vapors (TFA, conc. HCl, conc. HNO_3 , and HCOOH) for 5 min, the sensor turned yellow and emitted red light under UV irradiation (Figure 8a, S20). In contrast, no appreciable change was observed upon the vapors of neutral and basic organic solvents (Figure S21), demonstrating a good acid-selective response. The original yellow-green emission could be fully recovered followed by standing the acidified sensor in the ambient air for 1 h as the acid vapor volatilized, and the recovered sensor presented a similar response ability to TFA, which could be repeated many times with good reversibility (Figures 8b and S22). Thus, **TPBD-1** was prospective to fabricate a useful and recyclable sensing device to detect acid vapor via fluorescent and chromatic switching.

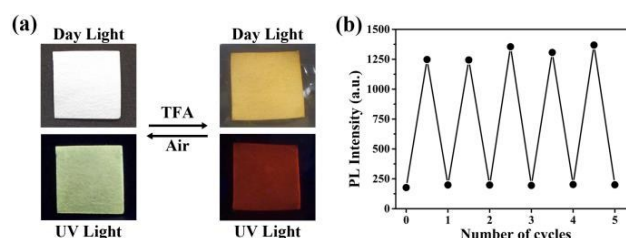


Figure 8. (a) Photographs of **TPBD-1** sensor fabricated on a piece of filter paper (size: 1 cm \times 1 cm) before and after fumed with TFA vapor under natural light (upper) and the illumination with 365 nm UV light (lower). (b) Fluorescence intensity of **TPBD-1** sensor as a function of the fuming–air cycle numbers. Excitation wavelength: 500 nm. The fluorescence intensity was monitored at the wavelength of 660 nm.

Taken the high sensitivity of fluorescent sensing into account, numerous AIEgens have been developed for acid detection by incorporation of various protonation sites, such as amino, alkylamine, and some nitrogen heterocyclic moieties.^{19,7b} The fluorescence emission of these conventional systems was commonly switched off under acid stimuli, due to the deaggregation of AIEgens or destruction of ICT process.^{3a} In this work, aryl substituted 1,4-enedione is evidenced to be a new candidate for proton binding with a quite disparate mechanism of acid-induced fluorescence, a prominently bathochromic shift in PL emission, as well as a great luminescence efficiency. More importantly, the switchable fluorescence color of **TPBD-1** (i.e., yellow-green for itself and red for its complex with TFA) is more favorable for optical sensing, since synchronous but inverse change in dual emission bands could self-calibrates the inaccuracies caused by photo bleaching, laser variations, and uneven labeling.²⁰ Therefore, aryl substituted 1,4-enedione based sensor possesses promising applications in acid detection and maybe other ratiometric evaluations.

Conclusions

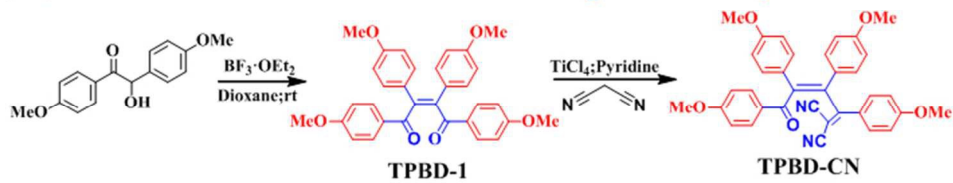
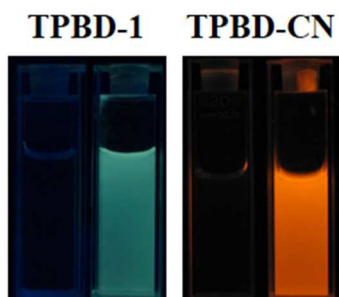
In summary, Z-selective aryl substituted 1,4-enediones have been designed, synthesized and demonstrated as a new class of versatile AIEgens with tunable fluorescence emission. Derivatization of 1,4-enedione with cyano unit led to an inherent D-A structure with enhanced AIE performance and pronounced red-emission. Moreover, the 1,4-enedione core could serve as a protonation site, and the reversible and stepwise complexation turned on a red emission by fixing molecular conformation and strengthening D-A interaction simultaneously. Based on that, the solid-state TPBD-1 sensor for TFA was fabricated, which presented switchable fluorescence color with good reversibility, implying a practical application in acid detection. The current study not only provides a new choice for the molecular design of AIEgens, but also paves the way to the development of functionally stimulus-responsive materials with colorful emissions.

Acknowledgements

Financial support by the National Natural Science Foundation of China (Grant 21522405 and 51503142), the Thousand Youth Talents Plan, and Natural Science Foundation of Tianjin (Grant 15JCYBJC52900) is gratefully acknowledged.

Notes and references

- (a) T. S. Qin, J. Q. Ding, M. Baumgarten, L. X. Wang and K. Müllen, *Macromol. Rapid Commun.*, 2012, **33**, 1036; (b) K. M. C. Wong and V. W. W. Yam, *Coordin. Chem. Rev.*, 2007, **251**, 2477; (c) D. D. Li, Y. P. Zhang, Z. Y. Fan, J. Chen and J. H. Yu, *Chem. Sci.*, 2015, **6**, 6097; (d) X. Y. Huang, S. Y. Han, W. Huang and X. G. Liu, *Chem. Soc. Rev.*, 2013, **42**, 173.
- T. Förster, K. Kasper, *Phys. Chem.*, 1954, **1**, 275.
- (a) J. Mei, N. L. C. Leung, R. T. K. Kwok, J. W. Y. Lam and B. Z. Tang, *Chem. Rev.*, 2015, **115**, 11718; (b) R. R. Hu, N. L. C. Leung and B. Z. Tang, *Chem. Soc. Rev.*, 2014, **43**, 4494; (c) J. Mei, Y. N. Hong, J. W. Y. Lam, A. J. Qin, Y. H. Tang and B. Z. Tang, *Adv. Mater.*, 2014, **26**, 5429; (d) J. Yang, J. Huang, Q. Q. Li and Z. Li, *J. Mater. Chem. C*, 2016, **4**, 2663; (e) D. Ding, K. Li, B. Liu and B. Z. Tang, *Acc. Chem. Res.*, 2013, **46**, 2441.
- (a) J. D. Luo, Z. L. Xie, J. W. Y. Lam, L. Cheng, H. Y. Chen, C. F. Qiu, H. S. Kwok, X. W. Zhan, Y. Q. Liu, D. B. Zhu and B. Z. Tang, *Chem. Commun.*, 2001, 1740; (b) Z. J. Zhao, B. R. He and B. Z. Tang, *Chem. Sci.*, 2015, **6**, 5347; (c) Z. J. Zhao, J. W. Y. Lam and B. Z. Tang, *J. Mater. Chem.*, 2012, **22**, 23726.
- Y. N. Hong, J. W. Y. Lam and B. Z. Tang, *Chem. Commun.*, 2009, 4332.
- (a) W. Z. Yuan, Y. Gong, S. Chen, X. Y. Shen, J. W. Y. Lam, P. Lu, Y. Lu, Z. Wang, R. Hu, N. Xie, H. S. Kwok, Y. Zhang, J. Z. Sun and B. Z. Tang, *Chem. Mater.*, 2012, **24**, 1518; (b) G. C. Yu, D. Wu, Y. Li, Z. H. Zhang, L. Shao, J. Zhou, Q. L. Hu, G. P. Tang and F. H. Huang, *Chem. Sci.*, 2016, **7**, 3017; (c) S. Dalapati, E. Q. Jin, M. Addicoat, T. Heine and D. L. Jiang, *J. Am. Chem. Soc.*, 2016, **138**, 5797; (d) Z. Y. Fan, D. D. Li, X. Yu, Y. P. Zhang, Y. Cai, J. J. Jin and J. H. Yu, *Chem. Eur. J.*, 2016, **22**, 3681; (e) M. Gao, L. C. Wang, J. J. Chen, S. W. Li, G. H. Lu, L. Wang, Y. J. Wang, L. Ren, A. J. Qin and B. Z. Tang, *Chem. Eur. J.*, 2016, **22**, 5107; (f) C. P. Ma, B. J. Xu, G. Y. Xie, J. J. He, X. Zhou, B. Y. Peng, L. Jiang, B. Xu, W. J. Tian, Z. G. Chi, S. W. Liu, Y. Zhang and J. R. Xu, *Chem. Commun.*, 2014, **50**, 7374;
- (g) C. Wang, B. J. Xu, M. S. Li, Z. G. Chi, Y. J. Xie, Q. Q. Li and Z. Li, *Mater. Horiz.*, 2016, **3**, 220. DOI: 10.1039/C7TC00173H
- (a) B. K. An, J. Gierschner and S. Y. Park, *Acc. Chem. Res.*, 2012, **45**, 544; (b) Z. Y. Yang, W. Qin, J. W. Y. Lam, S. J. Chen, H. H. Y. Sung, I. D. Williams and B. Z. Tang, *Chem. Sci.*, 2013, **4**, 3725; (c) B. Chen, H. Zhang, W. Luo, H. Nie, R. Hu, A. Qin, Z. Zhao and B. Z. Tang, *J. Mater. Chem. C*, 2017, **5**, 960.
- (a) S. Y. Li, X. B. Wang, N. Jiang and L. Y. Kong, *Eur. J. Org. Chem.*, 2014, 8035; (b) Q. H. Gao, Y. P. Zhu, M. Lian, M. C. Liu, J. J. Yuan, G. D. Yin and A. X. Wu, *J. Org. Chem.*, 2012, **77**, 9865.
- (a) C. Pierlot, V. Nardello, J. Schrive, C. Mabile, J. Barbillat, B. Sombret and J. M. Aubry, *J. Org. Chem.*, 2002, **67**, 2418; (b) J. M. Carney, R. J. Hammer, M. Hulce, C. M. Lomas and D. Miyashiro, *Synthesis*, 2012, **44**, 2560; (c) A. Parmar and H. Kumar, *Synthetic Commun.*, 2007, **37**, 2301; (d) T. Umezawa, Y. Sugihara, A. Ishii and J. Nakayama, *J. Am. Chem. Soc.*, 1998, **120**, 12351; (e) D. L. Wei and F. S. Liang, *Org. Lett.*, 2016, **18**, 5860.
- N. S. Gavande, S. Kundu, N. S. Badgular, G. Kaur and A. K. hakraborti, *Tetrahedron*, 2006, **62**, 4201.
- R. R. Hu, E. Lager, A. Aguilar-Aguilar, J. Z. Liu, J. W. Y. Lam, H. H. Y. Sung, I. D. Williams, Y. C. Zhong, K. S. Wong, E. Peña-Cabrera and B. Z. Tang, *J. Phys. Chem. C*, 2009, **113**, 15845.
- F. Bu, R. H. Duan, Y. J. Xie, Y. P. Yi, Q. Peng, R. R. Hu, A. J. Qin, Z. J. Zhao and B. Z. Tang, *Angew. Chem. Int. Ed.*, 2015, **54**, 14492.
- J. Liu, Q. Meng, X. T. Zhang, X. Q. Lu, P. He, L. Jiang, H. L. Don and W. P. Hu, *Chem. Commun.*, 2013, **49**, 1199.
- X. L. Luo, W. J. Zhao, J. Q. Shi, C. H. Li, Z. P. Liu, Z. S. Bo, Y. Q. Dong and B. Z. Tang, *J. Phys. Chem. C*, 2012, **116**, 21967.
- Y. Gong, G. Chen, Q. Peng, W. Z. Yuan, Y. Xie, S. Li, Y. Zhang and B. Z. Tang, *Adv. Mater.*, 2015, **27**, 6195.
- J. Mei, Y. N. Hong, J. W. Y. Lam, A. J. Qin, Y. H. Tang and B. Z. Tang, *Adv. Mater.*, 2014, **26**, 5429.
- M. J. Kamlet, J. L. M. Abboud, M. H. Abraham and R. W. Taft, *J. Org. Chem.*, 1983, **48**, 2877.
- H. X. Zhao, D. S. Guo and Y. Liu, *J. Phys. Chem. B*, 2013, **117**, 1978.
- (a) Y. Q. Dong, J. W. Y. Lam, A. J. Qin, Z. Li, J. Z. Liu, J. Z. Sun, Y. P. Dong and B. Z. Tang, *Chem. Phys. Lett.*, 2007, **446**, 124; (b) X. Cheng, D. Li, Z. Y. Zhang, H. Y. Zhang and Y. Wang, *Org. Lett.*, 2014, **16**, 880; (c) X. Cheng, Z. Y. Zhang, H. Y. Zhang, S. H. Han, K. Q. Ye, L. Wang, H. Y. Zhang and Y. Wang, *J. Mater. Chem. C*, 2014, **2**, 7385; (d) S. J. Chen, J. Z. Liu, Y. Liu, H. M. Su, Y. N. Hong, C. K. W. Jim, R. T. K. Kwok, N. Zhao, W. Qin, J. W. Y. Lam, K. S. Wong and B. Z. Tang, *Chem. Sci.*, 2012, **3**, 1804; (e) S. J. Chen, Y. N. Hong, Y. Liu, J. Z. Liu, C. W. T. Leung, M. Li, R. T. K. Kwok, E. G. Zhao, J. W. Y. Lam, Y. Yu and B. Z. Tang, *J. Am. Chem. Soc.*, 2013, **135**, 4926.
- (a) W. Pan, H. H. Wang, L. M. Yang, Z. Z. Yu, N. Li and B. Tang, *Anal. Chem.*, 2016, **88**, 6743; (b) M. H. Lee, J. H. Han, J. H. Lee, N. Park, R. Kumar, C. Kang and J. S. Kim, *Angew. Chem. Int. Ed.*, 2013, **52**, 6206; (c) T. S. Qin, J. Q. Ding, M. Baumgarten, L. X. Wang, K. Müllen, *Macromol. Rapid Commun.*, 2012, **33**, 1036.

(Z)-1,4-enediones: stereospecific synthesis**tunable AIE****acid sensing**